

Softlanding and STM imaging of Ag₅₆₁ clusters on a C₆₀ monolayer

S. Duffe¹, T. Irawan¹, M. Bielecki¹, T. Richter¹, B. Sieben¹, C. Yin², B. von Issendorff², M. Moseler^{3,4}, and H. Hövel^{1,a}

¹ Universität Dortmund, Experimentelle Physik I, 44221 Dortmund, Germany

² Universität Freiburg, Fakultät für Physik, Hermann-Herder Straße 3, 79104 Freiburg, Germany

³ Fraunhofer-Institut für Werkstoffmechanik IWM, Wöhlerstraße 11, 79108 Freiburg, Germany

⁴ Freiburg Materials Research Center, Stefan-Meier-Straße 21, 79104 Freiburg, Germany

Received 31 January 2007 / Received in final form 24 April 2007

Published online 20 June 2007 – © EDP Sciences, Società Italiana di Fisica, Springer-Verlag 2007

Abstract. The low energy deposition of silver cluster cations with 561 (± 5) atoms on a cold fullerene covered gold surface has been studied both by scanning tunneling microscopy and molecular dynamics simulation. The special properties of the C₆₀/Au(111) surface result in a noticeable fixation of the clusters without a significant change of the cluster shape. Upon heating to room temperature we observe a flattening or shrinking of the cluster samples due to thermal activation. Similar changes were observed also for mass selected Ag clusters with other sizes. For comparison we also studied Ag islands of similar size, grown by low temperature deposition of Ag atoms and subsequent annealing. A completely different behavior is observed with much broader size distributions and a qualitatively different response to annealing.

PACS. 68.37.Ef Scanning tunneling microscopy – 61.48.+c Fullerenes and fullerene-related materials – 61.46.-w Nanoscale materials

1 Introduction

For most applications that make use of the specific properties of mass-selected clusters it will be needed to immobilize the clusters on surfaces. In this respect it is crucial to obtain the same atom-by-atom accuracy for clusters deposited on surfaces as it is achieved regularly for clusters in gas phase. This is not trivial; even the verification that mass-selected clusters keep their size after deposition is not yet a standard experiment. For small clusters with just a few atoms the properties change significantly for each atom added; therefore in several experiments spectroscopic data was used for an indirect proof of successful mass selected deposition [1, 2]. A more direct measurement of the cluster sizes on the surface is made difficult by the low maximum cluster coverage which can be deposited without the risk of cluster coalescence. In principle scanning tunneling microscopy (STM) is an ideal tool for the direct study of the cluster sizes, but resolving the atomic structure of clusters on surfaces was up to now only possible in few cases, generally only for larger clusters with a low height/diameter ratio [3, 4]. For two-dimensional small clusters on a metal surface the determination of the cluster size with STM was only achieved using the skillful technique of a ‘rare gas necklace’, where the larger size and

more corrugated local density of states (LDOS) of the rare gas atoms decorating the rim of the clusters made a determination of the cluster size possible [5]. Without atomic resolution one has to be very careful in interpreting the STM results. It is well-known that the apparent width of clusters is always significantly increased by the finite curvature of the STM tip, which becomes obvious when in a single STM image quite dissimilar clusters appear to have identical lateral shapes [6, 7]. Double or multiple tip effects are often also present as well, so one has to check the STM images critically for multiple images of the same clusters, which is easier if the cluster coverage is not too large. In general it is assumed that at least particle heights as determined by STM are reliable. In the following, however, we will demonstrate that not even this is really justified. In addition to these imaging problems there exists the danger that the measured cluster size distribution is modified if some of the clusters get displaced by the STM tip instead of being imaged, which occurs with different probabilities for different cluster sizes. Therefore the clusters should be fixed to the surface sufficiently strongly enough to prevent displacement by the STM. On the other hand the interaction should not be too strong in order to avoid that the cluster structure changes completely upon deposition.

So the optimum surface for size-selected cluster deposition should be one with a weak, but noticeable interaction with the clusters. For imaging consequently

^a e-mail: hoevel@physik.uni-dortmund.de

low-temperature STM (LT-STM) will be required, since at room temperature (RT) thermally activated cluster diffusion and coalescence will occur for such rather weak cluster-surface interactions. In this report we will show that an Au(111) surface functionalized with a well ordered monolayer (ML) of C_{60} molecules seems to be close to such an ideal system. We chose this combination for several reasons. Stable STM imaging of Ag and Au islands on a C_{60} film has already been achieved [8–10]; in these studies three-dimensional islands were observed, which indicates that no strong wetting occurs. Nevertheless the stable imaging hints at some fixation of the clusters, which should at least partly be due to the corrugation of the C_{60} monolayer. This layer has a periodicity of about 1 nm and should therefore quite strongly hinder the movement of few nm particles. A further advantage of C_{60} films for cluster deposition is that with its intermolecular van der Waals-interaction it may induce some ‘soft-landing’ effect similar to rare gas films [1,11], even if the C_{60} -substrate interaction is stronger due to charge transfer effects [12]. Last but not least one can expect interesting charge transfer processes to occur between the clusters and the C_{60} film. Such processes have been discussed already for the Ag islands [9], and might lead to effects related to the particular properties of doped C_{60} films [13].

We have successfully deposited mass selected Ag cluster cations with 561 ± 5 atoms on 1 ML $C_{60}/Au(111)$; by low temperature STM imaging we could demonstrate that the clusters stay practically unchanged. We chose to deposit Ag_{561} since this cluster size corresponds to a ‘magic’ closed shell icosahedron [14], which should have an enhanced stability. One should note that it is actually not known yet whether silver clusters of this size really adopt an icosahedral structure. But as silver clusters up to size 79 clearly follow an icosahedral growth motif [15,16], and as it has been shown that for larger clusters icosahedral symmetry is at least one of the possible structures [17], it is highly probable that they do.

The experimental results are corroborated by an accompanying molecular dynamics study of Ag_{561} deposition using identical conditions as in the experiments.

2 Experimental and theoretical

For the cluster deposition we used a new set-up which consists of a magnetron-sputter gas aggregation cluster source [18], a very effective cryo-pump placed directly in the cluster beam [19] and a semi-continuous time-of-flight mass selector with high transmission and infinite mass range [20]. This cluster beam apparatus is connected to a surface science facility combining LT-STM and high-resolution photoemission [21]. A resolution of $m/\Delta m > 50$ and cluster currents of several ten pA (e.g. 93 pA for Ag_{55}^+) measured with a Faraday cup at the sample position are obtained in routine operation.

In Figure 1 we display one mass spectrum for clusters up to Ag_{70}^+ where we observe atom-by-atom mass resolution up to the largest size (Fig. 1a), and another spectrum

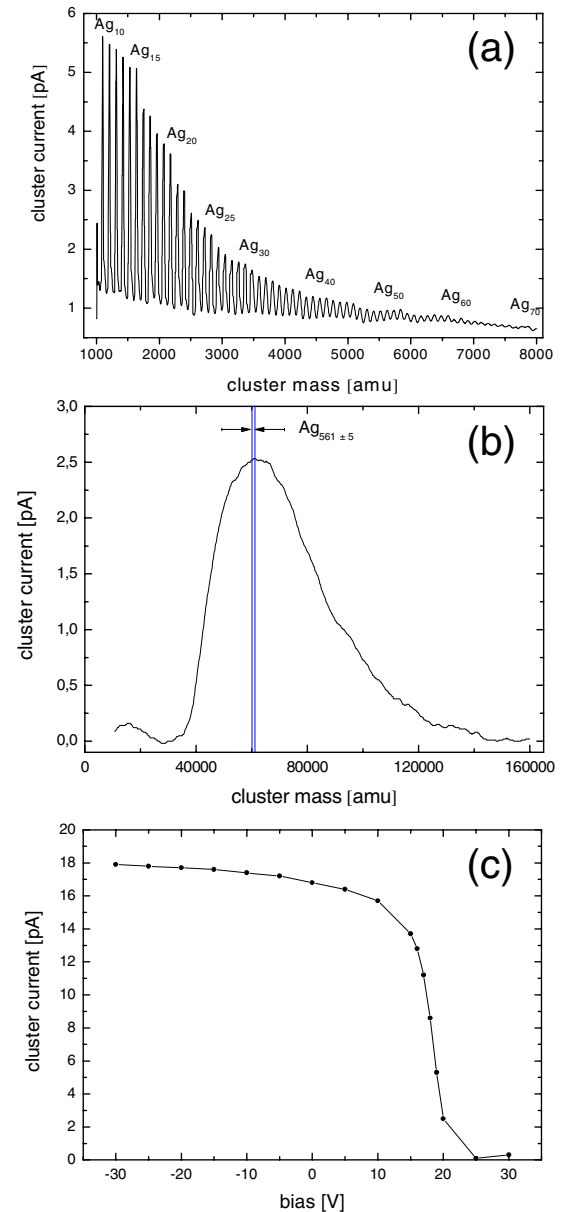


Fig. 1. (a) Mass spectrum measured for cluster cations with a Faraday cup at the sample position by variation of the pulses in the time-of-flight mass selector. With $m/\Delta m \approx 70$ we observe atom-by-atom mass selection up to Ag_{70} . (b) Mass spectrum measured with source parameters optimized for the production of larger clusters. The selection of $Ag_{561 \pm 5}$ is marked with two vertical lines. (c) Cluster current for Ag_{561}^+ versus bias voltage applied to the Faraday cup at the sample position. With 0 V bias the Ag_{561} clusters have a mean kinetic energy of ≈ 18 eV, i.e. 0.03 eV per atom.

which shows the cluster size distribution with cluster source parameters optimized for the production of larger clusters (Fig. 1b). Also in the latter case we select clusters with $m/\Delta m > 50$ as indicated in the graph. Before cluster deposition the cluster current is measured for different bias voltages (shown in Fig. 1c for Ag_{561}) and a sample bias for deposition is chosen which results in $\ll 0.1$ eV

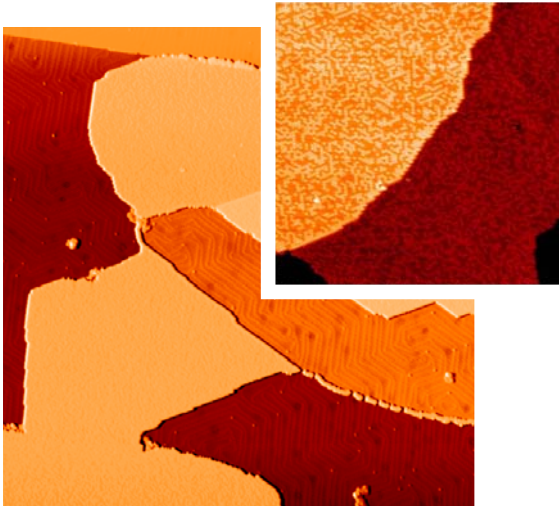


Fig. 2. STM images of an Au(111) surface partially covered with a C₆₀ monolayer, measured at $T = 77$ K. The large image (300×300 nm²) shows the large C₆₀ islands and the typical $23 \times \sqrt{3}$ reconstruction on the clean Au areas. The small inset (100×100 nm²) displays the structure of the C₆₀ film in detail.

kinetic energy per atom. The C₆₀ spacer layer may lead to a delayed electron transfer from the metal substrate to the cluster ions, as energy shifts in photoemission data for Ag islands on C₆₀/Si(111) suggest [9]. But the ion neutralization will be fast on the timescale of the deposition experiment since no static charging is observed in photoemission.

The deposition of Ag atoms for the comparative study of Ag island growth is realized with an evaporator with electron-beam heating and an integrated flux monitor. The evaporation rate is calibrated using either a quartz microbalance or more directly by island growth [22]. A sample bias is used to avoid the impact of Ag ions produced by the electron-beam heating. For both, Ag cluster and Ag atom deposition, the sample is mounted on a flow-through liquid helium cryostat, which can be operated at temperatures down to 10 K. For the preparation of a clean and well ordered surface either an Au(111) single crystal or an Au(111) film on mica is treated with several sputtering/heating cycles. A monolayer of C₆₀ is deposited using a quartz crucible with resistive heating instead of the evaporators with electron-beam heating, since the electron impact produces C_{60-2N} fragments, which show a completely different film growth [23] and therefore disturb the well ordered C₆₀ films. After C₆₀ deposition at RT, the sample is annealed at 250 °C, which results in well ordered monolayers. The structure of the C₆₀/Au(111) surface is always checked with LT-STM at 77 K before Ag cluster deposition or island growth. In Figure 2 we show an STM image with a coverage of less than one monolayer, where clean Au(111) areas coexist together with large, well ordered C₆₀ monolayers. Typically we obtain step-free areas of several 100 nm diameter.

In order to elucidate whether the experimental set-up allows for a softlanding of the silver clusters, we performed

a molecular dynamics study of the deposition of an Ag₅₆₁ cluster on an Au(111) surface covered by a fullerene monolayer. The potential energy surface of the Ag/C/Au system was modelled by the following analytic potentials. The metallic interactions (Ag-Ag, Au-Au and Ag-Au) were described by the Gupta many body potential [24]. Intra-fullerene forces were treated with the Tersoff potential [25] and the inter-fullerene (van der Waals) interactions with the Girifalco pair potential [26]. In order to parameterize the Ag-C and Au-C interaction, a Morse potential was fitted to the (ab-initio derived) equilibrium distance and adhesive energy of fullerenes adsorbed on Ag(111) and Au(111) surfaces [27], respectively, and to the experimental oscillation frequency of a fullerene charge shuttle between gold contacts [28]. Our model of the substrate consisted of a block of 9 Au(111) monolayers (with a lateral dimension 6.95 nm times 8.03 nm) covered by 64 C₆₀ molecules. Periodic boundary conditions were applied in the lateral directions. The lowest gold monolayer was held fixed while a Langevin thermostat was applied to the next 3 layers [29]. Prior to deposition, both the substrate and the icosahedral Ag₅₆₁ cluster were thermalized to the experimental temperatures $T_{substrate} = 165$ K and $T_{cluster} = 120$ K, respectively. The cluster trajectory was started 1 nm above the substrate with a kinetic energy of 18 eV (the experimental value) and the deposition dynamics was followed for 50 ps.

3 C₆₀ layer and Ag islands

As we are going to discuss the stability of silver particles on a C₆₀ layer for temperatures up to RT, we will first show results for the C₆₀/Au(111) system at RT and 77 K. In Figure 3a we present three images out of a larger series, which were measured with STM at RT consecutively at the same surface area. Recording one image took 22 min. As already described in the literature [12] the different heights, i.e. the bright or dark dots, are due to two different orientations of the C₆₀ molecules on the Au(111) surface. Localizing fixed positions one can align the frames and calculate the difference images (2-1) and (3-2). One clearly observes that most of the molecules have remained in the same orientation (grey areas) while a few have either turned from dark to bright (white dots) or from bright to dark (black dots). This change in orientation at RT is in agreement with the observations in reference [30]. In contrast, performing the same STM measurements at 77 K (cf. Fig. 3b) shows that the C₆₀ film is completely stable on a timescale of hours. One can therefore keep in mind that at RT the C₆₀ layer is a dynamic system, with some rotation of the molecules which might even enhance the diffusion of material on the layer, while at 77 K such effects can be safely neglected.

Let us turn now to the growth of Ag islands on the C₆₀ film. At a temperature <50 K an effective coverage of 0.3 ML of Ag atoms was evaporated on the C₆₀/Au(111) surface, hereafter the sample was transferred into the STM which was operated at 77 K. Figure 4a shows that small Ag islands with a mean height of about 0.4 nm are formed.

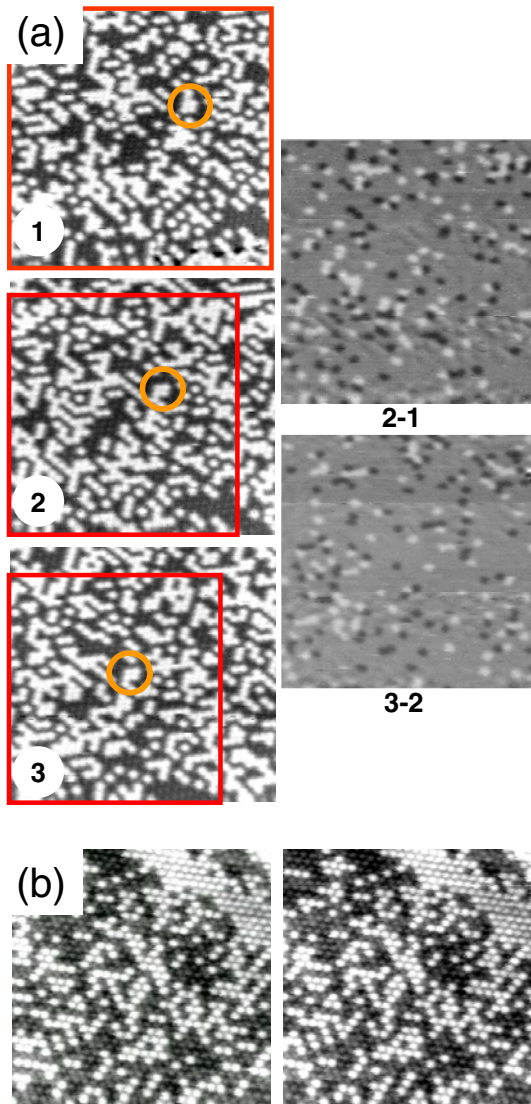


Fig. 3. (a) STM images ($33 \times 33 \text{ nm}^2$) of a C_{60} ML on Au(111), measured at RT. The images 1, 2 and 3 were measured sequentially. Recording one image took 22 min. The difference images (2-1) and (3-2) clearly show a change of the C_{60} orientation. (b) Two images ($33 \times 33 \text{ nm}^2$) measured at $T = 77 \text{ K}$ with 44 min in between. No change of the C_{60} ML is observed.

At 77 K the height distribution is stable at least on a timescale of more than 10 h. Subsequently the sample has been annealed at a number of different temperatures, each time for 45 min. First significant changes of the island height distribution occur if the sample is annealed at 165 K (Fig. 4b) which leads to the occurrence of larger island heights. With increase of the annealing temperature to 265 K (Fig. 4c) the island height further increases. After annealing at RT for 45 min, we checked also for the long term stability of the sample at RT on the timescale of more than 10 h.

The results of the complete series of annealing steps are summarized by the height distributions shown in Figure 5. The reproducibility of the height distributions for the

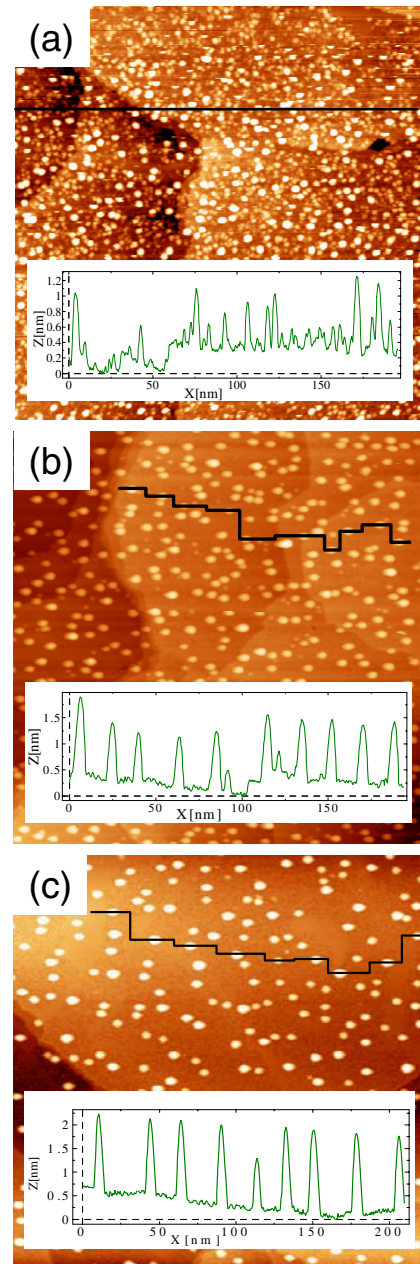


Fig. 4. STM images ($200 \times 200 \text{ nm}^2$) for Ag islands grown by Ag atom deposition on 1 ML $\text{C}_{60}/\text{Au}(111)$, measured at $T = 77 \text{ K}$. The insets show line profiles on the marked trajectories. Data taken for the following annealing steps: (a) directly after deposition at $T < 50 \text{ K}$; (b) sample annealed for 45 min at 165 K; (c) sample annealed for 45 min at 265 K.

same annealing temperature in two independent experimental runs was generally good. Some smaller variations are attributed to systematic errors due to the displacement of islands during STM imaging, which was not fully avoidable in particular for the small island sizes. Taking this variation into account we do not observe a significant change of the island height distribution for annealing temperatures below 165 K. Above 165 K the island height increases more and more up to RT, and there is an additional

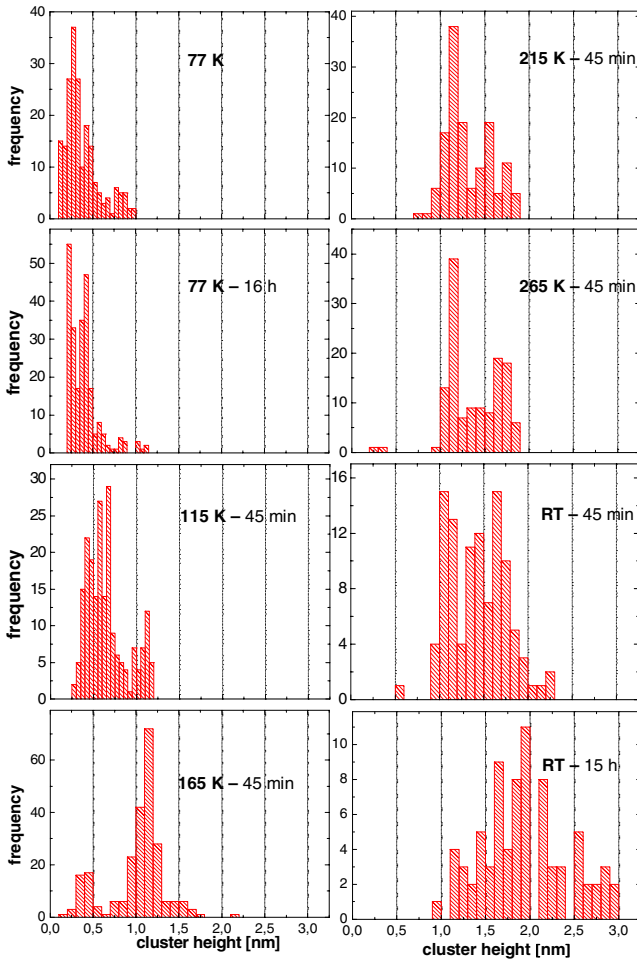


Fig. 5. Height distributions as measured for the Ag islands grown on 1 ML C₆₀/Au(111) for a number of different annealing steps. The total number of clusters varies between the different histograms. In addition to the \sqrt{N} statistical error for each bin also some systematic error due to clusters selectively displaced by the STM tip cannot be excluded (see text).

increase if we keep the sample at RT for 15 h. Calculating the effective Ag coverage, by assuming a spherical shape of the islands, neglecting the shape of the islands which may be also size dependent, one gets rather strongly varying values for the different annealing steps, which is probably again due to the systematic errors by cluster displacement as discussed above. But all in all the effective coverage is of the same order of magnitude, i.e. we do not observe a significant amount of material to disappear upon annealing of the sample.

4 Deposition of Ag₅₆₁

The results of Section 3 indicated that deposited clusters with a few hundred atoms should be stable for a substrate temperature of 165 K or below on the C₆₀/Au(111) substrate system. Since sample contamination by typical residual gas components in an UHV chamber is significantly reduced for temperatures above 100 K [31], we did

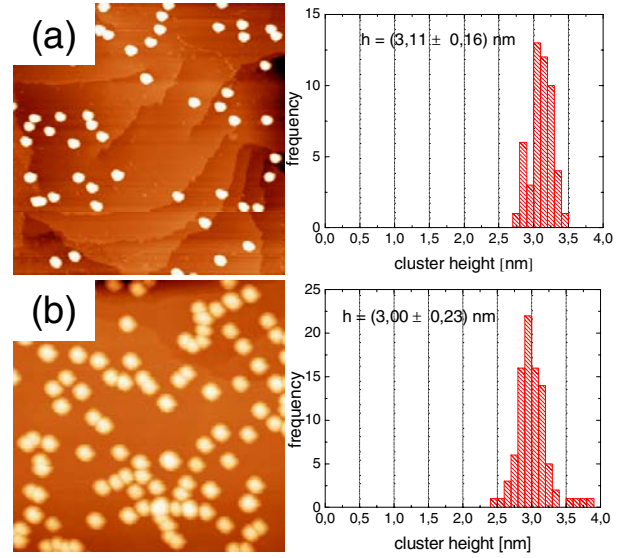


Fig. 6. STM images ($200 \times 200 \text{ nm}^2$) measured at $T = 77 \text{ K}$ of Ag₅₆₁ clusters deposited at $T = 165 \text{ K}$ on C₆₀/Au(111) (left) and the corresponding cluster height distribution as extracted from this image (right) for two different positions on the sample: (a) outer region of the deposition spot with low cluster coverage; (b) region in the center of the deposition spot with high cluster coverage. The different widths of the clusters in the STM images (a) and (b) are an example for the typical variations which are observed also on identical sample positions for different STM tip shapes. Tunneling parameters: $U_{\text{sample}} = +2.2 \text{ V}$, $I = 46 \text{ pA}$.

not use the minimal sample temperature achievable with our set-up, but instead used this temperature of 165 K for the deposition of Ag₅₆₁⁺ (in fact 561 ± 5 atoms) on C₆₀/Au(111). With a cluster current of 16 pA we deposited for a time interval of 10 min. With a sample bias of 0 V the clusters had a kinetic energy of 0.03 eV per atom (cf. Fig. 1c). After the deposition the sample was transferred within about 10 min into the STM operated at 77 K.

Two resulting STM images are shown in Figure 6. The STM image in Figure 6a was measured in the outer region of the deposition spot. Here the cluster coverage is low enough, that one could safely identify multiple cluster images due to tip artifacts, which, however, are not present in this image. Figure 6b is measured in the center of the deposition spot, where the cluster coverage is higher, about 90 clusters per $200 \times 200 \text{ nm}^2$. If one takes the cluster coverage of Figure 6b and the total number of 6×10^{10} clusters calculated from the cluster current and the deposition time, one gets a diameter of 5.8 mm for the deposition spot. This is in qualitative agreement with the width of the ion beam as roughly determined by lateral movement of the Faraday cup, which has a 3 mm diameter opening. On the right side the height distributions extracted from the STM images are shown. They are extremely narrow with a mean height of $\approx 3.1 \text{ nm}$ and a standard deviation of $\pm 0.2 \text{ nm}$. The slight differences between the height distributions of Figures 6a and 6b are within the statistical

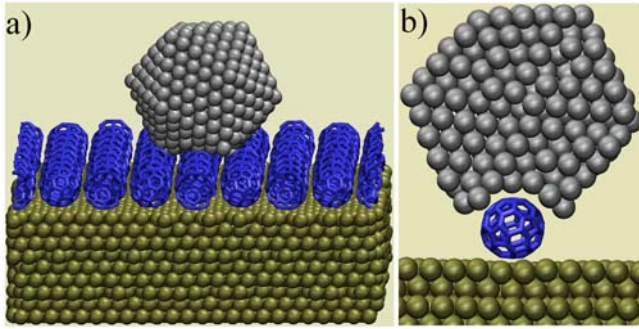


Fig. 7. Final configuration of a molecular dynamics simulation of Ag_{561} impinging on a gold supported monolayer of C_{60} . (a) Snapshot of the system after 50 ps. (b) A 0.8 nm thick slice of the cluster from (a) showing the wetting of the central fullerene (the other fullerenes are not shown) by the silver atoms. Silver atoms are depicted by grey spheres, the fullerenes by blue cages and the gold atoms are plotted in gold.

and systematic [32] errors of an STM measurement, which are estimated to 5%. The measured heights should be compared to the expected size of an Ag_{561} cluster. Assuming a spherical cluster shape with a volume of $V = (4/3)\pi(h/2)^3$ and taking the cluster volume as 561 times the atomic volume in bulk Ag one gets a height of $h = 2.64$ nm for Ag_{561} , which is significantly smaller than the experimental STM result. An even smaller value is obtained in the molecular dynamics simulation. Figure 7 displays the final configuration 50 ps after deposition. Although the cluster mainly kept its global icosahedral shape (Fig. 7a), structural damage can be observed in the vicinity of the carbon-silver interface (Fig. 7b). The distortion of the Ag_{561} can be explained by the relatively high adsorption strength of 1.5 eV [27] of the fullerenes to an Ag(111) surface resulting in the observed partial wetting of the fullerenes by the silver atoms. The resulting denticulation of the Ag_{561} and the fullerene layer (Fig. 7b) indicates strong friction forces for lateral motion of the silver clusters corroborating the experimental observation that the clusters are not displaced during the scanning with the STM. The geometrical height of the cluster was calculated as the vertical (z -) distance between the highest atom of the fullerene layer and the highest silver atom. A value of 2.3 nm is obtained, again considerably smaller than the experimental (STM-derived) value of 3.1 nm. In order to check the sensitivity of the final cluster height to variations in the Ag-C interaction strength an additional simulation using the weaker (Lennard-Jones type) interaction of Garrison and coworkers [33] was carried out. Although the wetting was less pronounced, the final height of the silver cluster turned out to be essentially the same as calculated with the stronger interaction.

These findings clearly point out difficulties in the use of an STM to determine cluster heights in heterogeneous cluster-surface systems, which here are probably due to the different LDOS contours of the cluster and the C_{60} surface. We are going to investigate these effects in detail in the near future by measuring heights of different cluster sizes and materials as well as by performing density

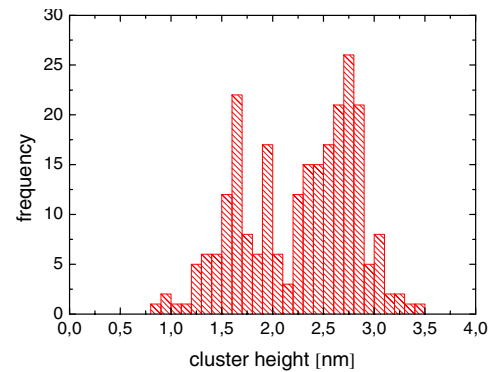
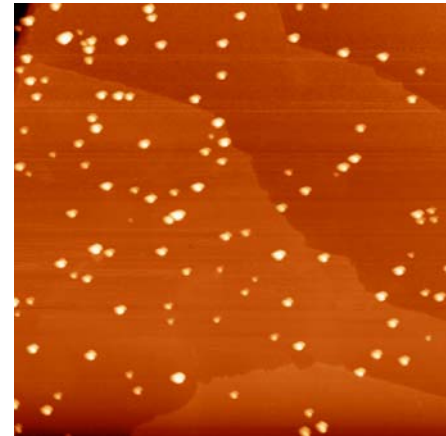


Fig. 8. STM image ($300 \times 300 \text{ nm}^2$) and a corresponding height distribution after annealing the sample with Ag_{561} clusters on $\text{C}_{60}/\text{Au}(111)$ for 45 min at RT. The cluster heights have decreased with one maximum of the distribution at about 2.6 nm but also a significant accumulation around 1.6 nm. Tunneling parameters: $U_{\text{sample}} = +2.3$ V, $I = 46$ pA.

functional simulations. We would like to stress again that for the cluster size determination the measured width without resolution of the cluster shape does not represent an alternative, since it includes the tip shape, which is generally changing from measurement to measurement (cf. Fig. 6) and eludes an experimental determination. Nevertheless, despite the discrepancy between the measured and the calculated cluster heights, the extremely narrow height distribution observed makes us confident that what we are seeing in Figure 6 are indeed $\text{Ag}_{561 \pm 5}$ clusters deposited without coalescence or fragmentation or even strong shape changes. To our knowledge such STM imaging of softlanded size selected clusters has not yet been demonstrated before, at least not for clusters of several 100 atoms.

In order to check the stability of the deposited clusters, we subsequently annealed the sample in the same way as for the Ag island samples at 215 K, 265 K and RT, each time for 45 min. Below RT we do not observe a significant change of the cluster height distribution. After 45 min at RT, however, the cluster heights have significantly decreased, as shown in Figure 8. This is in sharp contrast to the increase of the Ag island heights after annealing as described above (cf. Fig. 5). Another qualitative difference

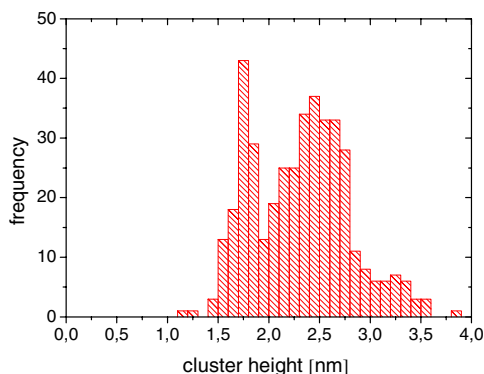


Fig. 9. Cluster height distribution for Ag₅₆₁ clusters deposited on C₆₀/Au(111) taken from a separate set of experiments with deposition at RT. After the deposition it took about 45 min to transfer the sample into the STM where the sample was imaged at 77 K. The similarity to Figure 8 is obvious.

is that the effective Ag coverage is significantly decreased, because the number of clusters per area is constant or even lower than before annealing. In Figure 8 we show a typical STM image of the sample and the corresponding height distribution. It is obvious that this distribution has some substructure, with one maximum at about 2.6 nm, but also a significant accumulation for cluster heights around 1.6 nm.

This two-peak structure of the height distribution is clearly corroborated by the height distribution in Figure 9, which was measured for Ag₅₆₁ clusters deposited at RT and transferred into the 77 K STM, after about 45 min. Actually, RT depositions were the first experiments done. Already a broad range of cluster sizes has been studied and a sharp maximum in the cluster height distribution at about 1.7 nm was observed also for other cluster sizes deposited at RT [34]. At least for Ag_{309 ± 3} with an initial height of (2.6 ± 0.2) nm after deposition at 165 K recent experiments confirm the decay of the cluster height at RT and the appearance of a sharp maximum at 1.7 nm. This demonstrates that thermally activated processes shrink the clusters to 1.7 nm height, which might indicate a metastable ‘magic’ cluster size on the surface. We will discuss this in detail in a separate publication. Even for the annealed Ag islands one can observe similar substructures with multiple maxima in the height distributions.

Keeping the samples with the Ag₅₆₁ clusters deposited at 165 K for 15 h at RT finally leads to the disappearance of almost all of the clusters. Only in the areas in the center of the deposition spot (cf. Fig. 6b) some small clusters remained. The STM image in Figure 10 shows that during this process the structure of the C₆₀/Au(111) substrate is changed. Small islands of about 0.3 nm height appear which were not present before the cluster decay. We can explain this, if we assume that the Ag material penetrates the C₆₀ film at RT and forms small Ag islands below the film or incorporated in the Au(111) substrate. We mention that we observed a similar disappearance of the clusters also for Ag₃₀₉ clusters, if we kept the sample at RT for

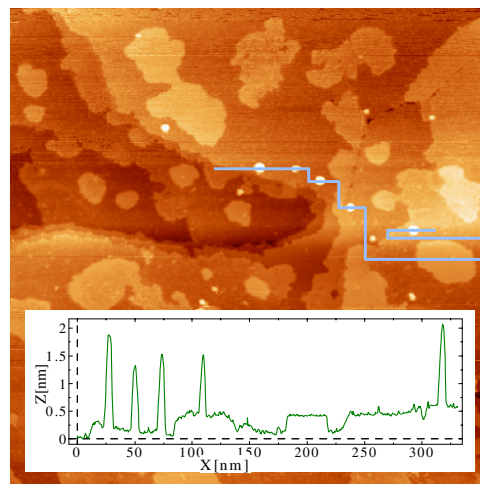


Fig. 10. STM image (300 × 300 nm²) measured at $T = 77$ K and a line profile (inset) on the marked trajectory for Ag₅₆₁ clusters deposited on 1 ML C₆₀/Au(111) after annealing the sample 15 h at RT. Almost all clusters have disappeared and small islands with 0.3 nm height appear in the C₆₀ layer.

12 h. It is important to notice that again the behavior is qualitatively different compared to the Ag islands, where we did not notice a significant decrease of the effective Ag coverage if we kept the sample at RT; instead the Ag material reorganized into larger islands.

5 Conclusions

We have shown that it is possible to softland mass selected Ag_{561 ± 5} clusters on an Au(111) surface functionalized with an ordered ML of C₆₀ molecules. This substrate system proved to be a new and promising choice for the investigation of mass selected clusters attached to a surface. Stable cluster samples could be obtained for deposition at a temperature of 165 K, which in the STM images measured at 77 K gave an extremely narrow height distribution with (3.1 ± 0.2) nm cluster height. Molecular dynamics simulations of the deposition suggest that the experimental conditions indeed are close to softlanding with only minor distortions of the Ag₅₆₁ icosahedra occurring at the cluster-fullerene interface. After annealing the samples up to RT we observed thermally activated cluster decay and penetration of the Ag material through the C₆₀ film. We compared these data with results which we obtained for Ag islands produced by the deposition of Ag atoms at low temperatures and subsequent annealing. In this case the Ag material reorganizes into larger islands for annealing up to RT, which is in sharp contrast to the cluster decay for the deposited clusters. As a very interesting additional observation we mention the appearance of a sharp maximum at about 1.7 nm cluster height during the decay of the deposited clusters. This seems to be an indication for some ‘magic’ cluster size in the cluster-surface system.

This work was supported by the Deutsche Forschungsgemeinschaft (SPP 1153 and GK 726).

References

1. S. Fedrigo, W. Harbich, J. Buttet, Phys. Rev. B **58**, 7428 (1998)
2. J.T. Lau, H.-U. Ehrke, A. Achleitner, W. Wurth, Low Temp. Phys. **29**, 223 (2003)
3. A. Piednoir, E. Perrot, S. Granjeaud, A. Humbert, C. Chapon, C.R. Henry, A. Piednoir, A. Humbert, C. Chapon, C.R. Henry, E. Perrot, S. Granjeaud, Surf. Sci. **391**, 19 (1997)
4. K.H. Hansen, T. Worren, S. Stempel, E. Laegsgaard, M. Bäumer, H.-J. Freund, F. Besenbacher, I. Stensgaard, Phys. Rev. Lett. **83**, 4120 (1999)
5. R. Schaub, H. Jödicke, F. Brunet, R. Monot, J. Buttet, W. Harbich, Phys. Rev. Lett. **86**, 3590 (2001)
6. H. Hövel, Th. Becker, A. Bettac, B. Reihl, M. Tschudy, E.J. Williams, J. Appl. Phys. **81**, 154 (1997)
7. H. Hövel, Appl. Phys. A **72**, 295 (2001)
8. Zhao Y. Rong, L. Rokhinson, Phys. Rev. B **49**, 7749 (1994)
9. M.D.R. Taylor, P. Moriarty, B.N. Cotier, M.J. Butcher, P.H. Beton, V.R. Dhanak, Appl. Phys. Lett. **77**, 1144 (2000)
10. Haiqian Wang, J.G. Hou, O. Takeuchi, Y. Fujisuku, A. Kawazu, Phys. Rev. B **61**, 2199 (2000)
11. H. Cheng, U. Landman, Science **260**, 1304 (1993)
12. E.I. Altman, R. Colton, Phys. Rev. B **48**, 18244 (1993)
13. A.F. Hebard, M.J. Rosseinsky, R.C. Haddon, D.W. Murphy, S.H. Glarum, T.T.M. Palstra, A.P. Ramirez, A.R. Kortan, Nature **350**, 600 (1991)
14. T.P. Martin, Phys. Rep. **273**, 199 (1996)
15. H. Häkkinen, M. Moseler, O. Kostko, N. Morgner, M. Astruc Hoffmann, B. von Issendorff, Phys. Rev. Lett. **93**, 093401 (2004)
16. M.N. Blom, D. Schooss, J. Stairs, M. Kappes, J. Chem. Phys. **124**, 244308 (2006)
17. B.D. Hall, M. Flüeli, R. Monot, J.-P. Borel, Phys. Rev. B **43**, 3906 (1991)
18. H. Haberland, M. Mall, M. Moseler, Y. Qiang, Th. Reiners, Y. Thurner, J. Vac. Sci. Technol. A **12**, 2925 (1994)
19. H. Hövel, S. Fritz, A. Hilger, U. Kreibig, M. Vollmer, Phys. Rev. B **48**, 18178 (1993)
20. B. von Issendorff, R.E. Palmer, Rev. Sci. Instrum. **70**, 4497 (1999)
21. H. Hövel, T. Becker, D. Funnemann, B. Grimm, C. Quitmann, B. Reihl, J. Electron Spectrosc. Relat. Phenom. **88-91**, 1015 (1998)
22. T. Irawan, I. Barke, H. Hövel, Appl. Phys. A **80**, 929 (1005)
23. D. Löffler, S.S. Jester, P. Weis, A. Böttcher, M.M. Kappes, J. Chem. Phys. **124**, 054705 (2006)
24. A. Rapallo, G. Rossi, R. Ferrando, A. Fortunelli, B.C. Curley, L.D. Lloyd, G.M. Tarbuck, R.L. Johnston, J. Chem. Phys. **122**, 194308 (2005)
25. J. Tersoff, Phys. Rev. Lett. **56**, 632 (1986); J. Tersoff, Phys. Rev. B **39**, 5566 (1989)
26. L.A. Girifalco, J. Phys. Chem. **96**, 858 (1992)
27. L.-L. Wang, H.-P. Cheng, Phys. Rev. B **69**, 165417 (2004)
28. H. Park, J. Park, A.K.L. Lim, E.H. Anderson, A.P. Alivisatos, P.L. McEuen, Nature **407**, 57 (2000)
29. M. Moseler, J. Nordiek, H. Haberland, Phys. Rev. B **56**, 15439 (1997)
30. E.I. Altman, R.J. Colton, Surf. Sci. **295**, 13 (1993)
31. M. Wutz, H. Adam, W. Walcher, *Theory and practice of vacuum technology* (Vieweg and Son, 1989)
32. L.E.C. van de Leemput, P.H.H. Rongen, B.H. Timmermann, H. van Kempen, Rev. Sci. Instrum. **62**, 989 (1991)
33. R. Chatterjee, Z. Postawa, N. Winograd, B. Garrison, J. Phys. Chem. B **103**, 151 (1999)
34. T. Irawan, Ph.D. thesis, Universität Dortmund, 2006